

Article

# Effect of the Addition of Rare Earth Element La on the Tribological Behaviour of AlSi5Cu1Mg Alloy

Wei Liu <sup>1,2</sup>, Hong Yan <sup>1,2,\*</sup> and Jian-Bin Zhu <sup>1,2</sup>

<sup>1</sup> School of Mechanical Electrical Engineering, Nanchang University, Nanchang 330031, China; chentailiu@outlook.com (W.L.); jianbinzhu1982@tom.com (J.-B.Z.)

<sup>2</sup> Key Laboratory of Light Alloy Preparation & Processing, Nanchang University, Nanchang 330031, China

\* Correspondence: hyan@ncu.edu.cn; Tel.: +86-791-8396-9633; Fax: +86-791-8396-9622

Received: 15 December 2017; Accepted: 22 January 2018; Published: 24 January 2018

**Abstract:** The effects of 0, 0.3, 0.6 and 0.9 wt % modifier La on the dry sliding wear behaviours of AlSi5Cu1Mg alloy were investigated under different friction conditions (normal loads, sliding velocities) by using pin-on-disc configuration. The microhardness of the alloys was tested, and it was found that the microhardness of the alloys was improved by the La addition. The AlSi5Cu1Mg + 0.6 wt % La alloy exhibited the smallest grain size and maximum microhardness. The wear mechanism analysis of the worn surface was done, which drew support from a scanning electron microscope (SEM) that was equipped with an energy dispersive spectrometer. The results showed that AlSi5Cu1Mg + 0.6 wt % La alloy exhibited the best wear resistance, which was mainly due to the modified grain and microhardness. At the sliding velocity of 0.19 m/s, the adhesive wear became the main wear mechanism with the increase of the load because of the rupture of the oxide layer on the friction surface. Under the load of 3.8 MPa, the abrasive wear became slight as the sliding velocity increasing, due to the recrystallization phenomenon that happened in the frictional surface.

**Keywords:** AlSi5Cu1Mg; La; microhardness; wear resistance

## 1. Introduction

Due to the low density and high mechanical properties, aluminium alloy attracted much interest in the field of automotive lightweight application [1]. However, wear and tear of aluminium alloy is a very serious problem in engineering applications such as transmission parts of automobiles [2–5]. Machine parts are often damaged directly or indirectly due to mechanical damage caused by wear. In addition, wear and tear can expand the tolerances of mating parts and damage the surface roughness, resulting in components replacement and severely shortening the service life of parts. Although aluminium alloy is widely used in panel structure because of the excellent mechanical properties, its poor wear resistance is a serious hindrance against wider application. Lots of works were completed by researchers to improve the wear resistance of aluminium alloys [6,7]. Recently, many secondary phases have been added into aluminium alloys to fabricate aluminium matrix composites with high wear resistance [8–11]. Altinkök [12] reported that fine Al<sub>2</sub>O<sub>3</sub>/SiC particles were propitious to the effects on the tribological properties of Al-based composite. Selvi et al. [13] found that the fly ash particles improved the wear resistance of the aluminium based metal matrix composites because the hardness of composites increased as the fly ash content was increased. Ficici et al. [14] investigated that situ AlB<sub>2</sub> reinforced Al-4Cu metal matrix composite exhibited better wear resistance and lower friction coefficient to varying degrees of magnitudes. Even so, a drawback of aluminium alloy matrix composite is that the reinforcement phase makes machining of components difficult [15]. However, rare earth modification is not the case.

Rare earth elements are called “vitamins” in metals, and their metal activity is second only to alkali metals and alkaline earth metals. Adding a small amount of rare earth to the metal can

greatly improve the performance of the metal [16]. Many studies have shown that rare earth element modification can effectively improve the comprehensive mechanical properties of aluminium alloys [17, 18]. Qiu et al. [19] investigated the modification of near-eutectic Al-12Si alloys with samarium and found that a good mechanical performance of the upgrade has been obtained when the addition of Sm was up to 0.6 wt %. Kaur et al. [20] studied the influences of electromagnetic stirring and rare earth addition on reciprocating wear behaviour of hypereutectic Al-Si alloys and found that the process has significantly decreased the wear rates of alloys.

It has been investigated that the variation of in friction and the wear rate strongly depends on the normal load, geometry of specimens, relative surface motion, sliding velocity, surface roughness, alloy chemistry, system rigidity, temperature exposed relative humidity, lubrication, vibration, etc. Among them, the sliding velocity and the normal load are the two important factors that play a significant role in the variation of tribological behaviour of materials under study [21,22]. Yan et al. [23] investigated the wear behaviour of co-continuous Al-23Si/SiC composites, which were performed within a load range of 5–25 N and a sliding velocity range of 100–200 r/min. Uyyuru et al. [24] performed testes on Al-Si-SiCp composites and reported that the wear rate and friction coefficients were observed to vary proportionally with the sliding speed. In one word, it is important to develop the rare earth aluminium alloys that have excellent wear resistance.

The aim of this investigation was to characterize the effect of rare earth element La content on the wear behaviour of AlSi5Cu1Mg alloy. Furthermore, the wear behaviour of alloys was tested under normal loads of 1.3, 3.8, 6.3 MPa and sliding velocity of 0.19, 0.57 m/s using pin-on-disc configuration against a steel disc counter-body. The wear morphology of the worn surface was studied using scanning electron microscope (SEM).

## 2. Experimental

The material employed in the current work was commercial AlSi5Cu1Mg (Table 1) alloy and modified alloys containing 0.3, 0.6 and 0.9 wt % of La. The details of this process were as follows: four alloys with the basic composition of AlSi5Cu1Mg alloy at 1053 K were melted in a quartz crucible inside a furnace for 45 min. In addition, three of the melts were added with 0.3 wt %, 0.6 wt % and 0.9 wt % La (in the form of Al-10 wt % La master alloy).

**Table 1.** Main chemical composition of the AlSi5Cu1Mg alloy (wt %).

Si	Mg	Cu	Zn	Fe	Mn	Al
4.5~5.5	0.4~0.6	1.0~1.5	<0.3	0.6~1.0	<0.5	Balance

The microstructures of the alloys were observed by optical microscopy (Eclipse MA200, Nikon Metrology, Inc., Brighton, UK). The microstructural evolution, morphological changes in the compounds and effect of La addition were also investigated. Vickers hardness of casting samples was obtained by using the HV 1000 A hardness tester device (Laizhou Huayin Testing Instrument Co., Ltd., Laizhou, China). The sample was cut using a spark wire-cutting machine to make a small cylinder with a diameter and a height of 10 mm. The parallelism between the measured surface and the bottom surface is less than 0.01 mm. The measured surface of the sample was polished to a roughness less than 0.1  $\mu\text{m}$ . The samples were tested at room temperature. The sample was tested ten times on a selection of different region loading forces of 200 gf successively, and the loading positions (black prism) were shown in Figure 1a. It took 15 s to load the sample each time. Finally, a corresponding experimental report was generated.

The tribological properties were determined in MMD-1 (Jinan Yihua Tribology Testing Technology Co., Ltd., Jinan, China) pin-on-disc apparatus at an ambient temperature of  $25 \pm 3$  °C. The wear tests were performed in a laboratory atmosphere with a relative humidity ranging from 40% to 60%. The wear tests were performed by the method known as unidirectional sliding pin on disc, where a pin

was spun clockwise relative to the disc by the rotation radius of 18 mm, and all the tests were carried out without introducing any lubricant into the contact area. The wear test was shown in Figure 1b schematically. Castings were machined into 4.5 mm diameter and 11 mm length pins. C45E4 steel with a hardness of 55 HRC was used as the rotating disc. Prior to each test, the pin and disc surfaces were ground with 2000-grit SiC abrasive paper and cleaned in ethanol using an ultrasonic device. Wear tests were conducted with normal loads of 20, 60 and 100 N (respectively equivalent to 1.3, 3.8 and 6.3 MPa) meanwhile operating with sliding velocity of 100 and 300 r/min (equivalent to 0.19 and 0.57 m/s, respectively) for 10 min. The real-time friction coefficient can be generated directly from the MMD-1 device. The worn surface was studied by a scanning electron microscope (SEM, VEGA3, TESCAN CHINA, Ltd., Shanghai, China) with an energy dispersive spectrum (EDS). Before the scanning, the pins have been cleaned in ethanol using an ultrasonic device for 5 min. The weight loss of the samples was obtained by weighing the pin before and after each test using FA2204B electronic balance, and converted to volume loss by using the density of each sample.

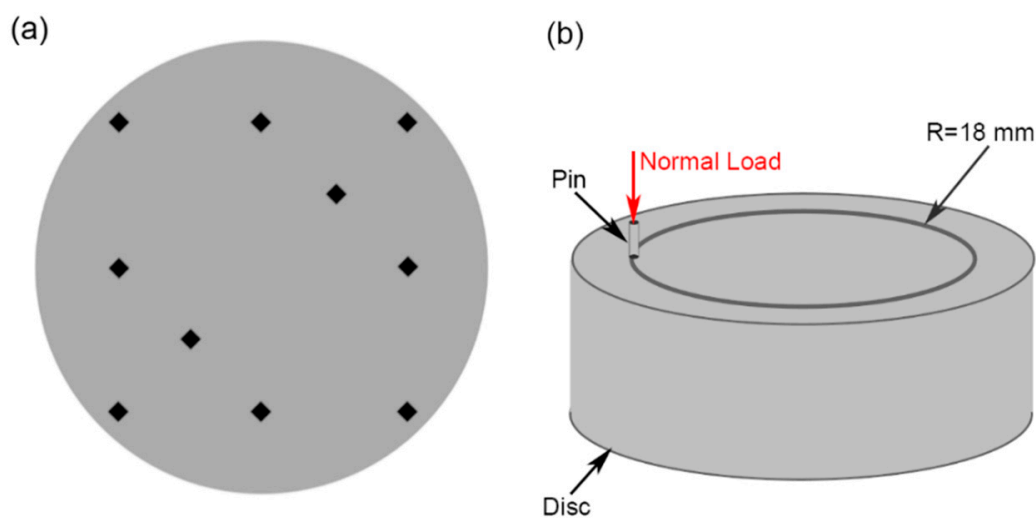


**Figure 1.** (a) the loading positions (black prism) of wear test; (b) the wear test in pin-on-disc apparatus.

### 3. Results and Discussion

#### 3.1. Microstructure and Microhardness

Optical micrographs of AlSi5Cu1Mg alloy samples with different contents of La are shown in Figure 2. It can be concluded that, with the adding of the content of La, there is a significant difference in the grain refinement effect. The microstructure of as-cast AlSi5Cu1Mg alloy consists of a wide range of intermetallic phases such as  $\alpha$ -Al,  $Al_4Fe$ ,  $\gamma-Al_3FeSi$ ,  $\alpha-Al_8Fe_2Si$ ,  $\beta-Al_5FeSi$  and  $Al_{12}FeMnSi$  phase [25]. The matrix  $\alpha$ -Al of as-cast AlSi5Cu1Mg alloy exhibits coarse dendrites and irregular shapes of clutter (Figure 2a). With the addition of La, the contour of the matrix  $\alpha$ -Al becomes clearer and the shape becomes more regular. When the addition amount of La was 0.6 wt %, the dendrites disappeared, and the grains became small and round. In addition, the matrix  $\alpha$ -Al distribution is more uniform (Figure 2c). In contrast to Figure 2c,d, it can be seen that, if the amount of La increased to 0.9 wt %, the matrix  $\alpha$ -Al began to coarsen and be converted into slats. Additionally, with the increase in the amount of La, elongated eutectic silicon gradually becomes shorter and smoother without edges and corners. Furthermore, when the addition amount of La was 0.6 wt %, eutectic silicon was converted into granular form.

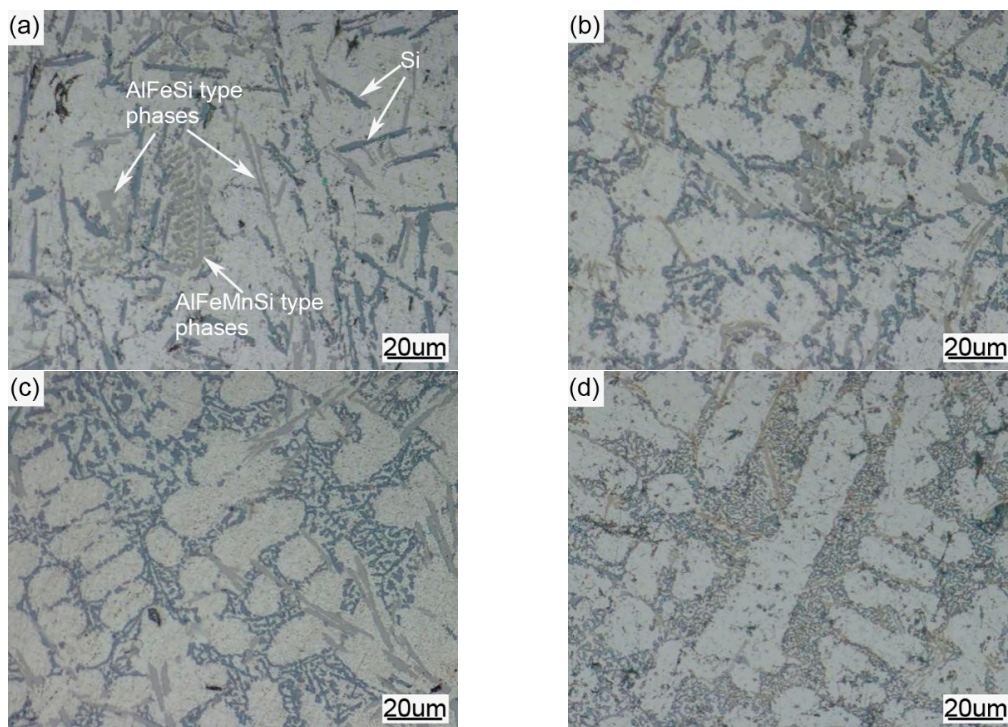


**Figure 2.** Microstructures of AlSi5Cu1Mg alloy samples with different contents of La: (a) 0 wt %, (b) 0.3 wt %, (c) 0.6 wt % and (d) 0.9 wt %.

With La was added to AlSi5Cu1Mg alloy, the size of the AlFeMnSi type phases in the coarse skeleton of the alloy were reduced, and the angular and needle-like AlFeSi type phases were refined into short rods or granules. This metamorphic effect can be attributed to the surface activity of rare earth elements. After the RE was added as the form of La rich master metal, a rod like  $Al_{11}RE_3$  ( $Al_4RE$ ) intermetallic phase [26] was observed in the microstructure. The SEM micrograph of AlSi5Cu1Mg + 0.6 wt % La alloy is shown in Figure 3a. In addition, the EDS spectrum of the precipitates (region A in Figure 3a) is shown in Figure 3b. The analysis revealed that the precipitates could be  $Al_{11}La_3$  phase. The  $Al_{11}La_3$  phase has a high thermal stability and can improve the mechanical properties of AlSi5Cu1Mg alloy [27]. It also can promote wear resistance. Asl et al. [28] have reported about the positive role played by  $Al_{11}RE_3$  particles in the wear resistance of AZ91 alloy at high loads.

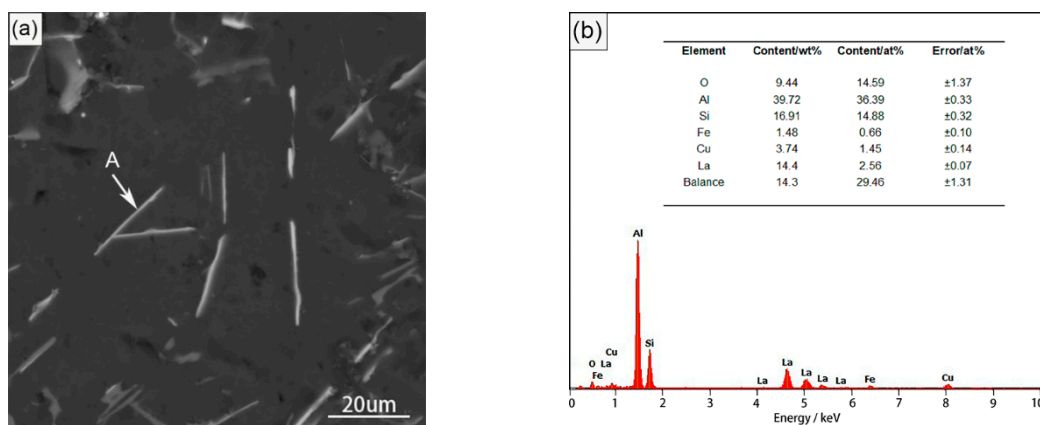


**Figure 3.** Scanning electron microscope (SEM) micrograph of (a) AlSi5Cu1Mg + 0.6 wt % La alloy and (b) energy dispersive spectrum (EDS) analysis of region A in (a).

The microhardness and the grain size of the alloys are shown in Figure 4. It indicated that the microhardness of the AlSi5Cu1Mg + 0.6 wt % La was 34% higher than that of the matrix alloy. However, further addition of modifier resulted in decrease microhardness values. According to the Hall–Petch Equation (1) [29,30]:

$$\sigma_y = \sigma_0 + \frac{k_y}{\sqrt{d}}, \quad (1)$$

where  $\sigma_y$  is the yield load (It can be expressed by microscopic Vickers hardness [31].),  $\sigma_0$  is a materials constant for the starting load for dislocation movement (or the resistance of the lattice to dislocation motion),  $k_y$  is the strengthening coefficient (a constant specific to each material), and  $d$  is the average grain diameter. The finer grain of the alloy, the higher strength and the greater hardness of the alloy. The alloy with 0.6 wt % La had the highest microhardness due to its smallest and regular grains. However, increasing the content of La to 0.9 wt %, the microhardness of alloy decreased. This could be due to the fact that AlSi5Cu1Mg alloy contains a variety of alloying elements. If the amount of rare earth added to the alloy exceeds a certain value, the rare earth element will be enriched at the front of the solidification interface (it is shown in Figure 5) and prevent the diffusion of other alloying elements into the solid phase, then reduce the solid solubility of alloy elements in matrix  $\alpha$ -Al, make the number of eutectic increase, cause segregation and reunion, hinder the refinement effect, and make the organization begin to deteriorate. Furthermore, Pournabari [32] reported that, at a higher La levels, the new La-rich intermetallic (AlSiLa intermetallic) slows the growth rate of the  $\alpha$ -Al primary phase. It reduced the strengthening phase of the alloy.

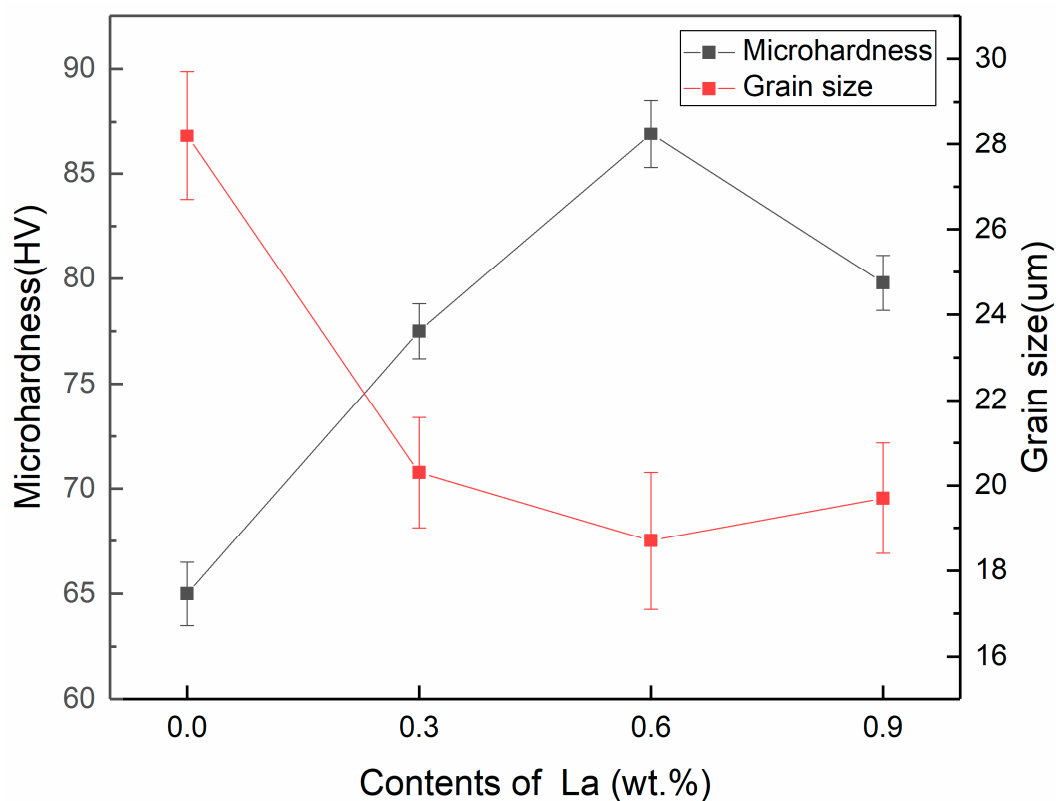


Figure 4. Microhardness and grain size of AlSi5Cu1Mg alloys with different contents La.

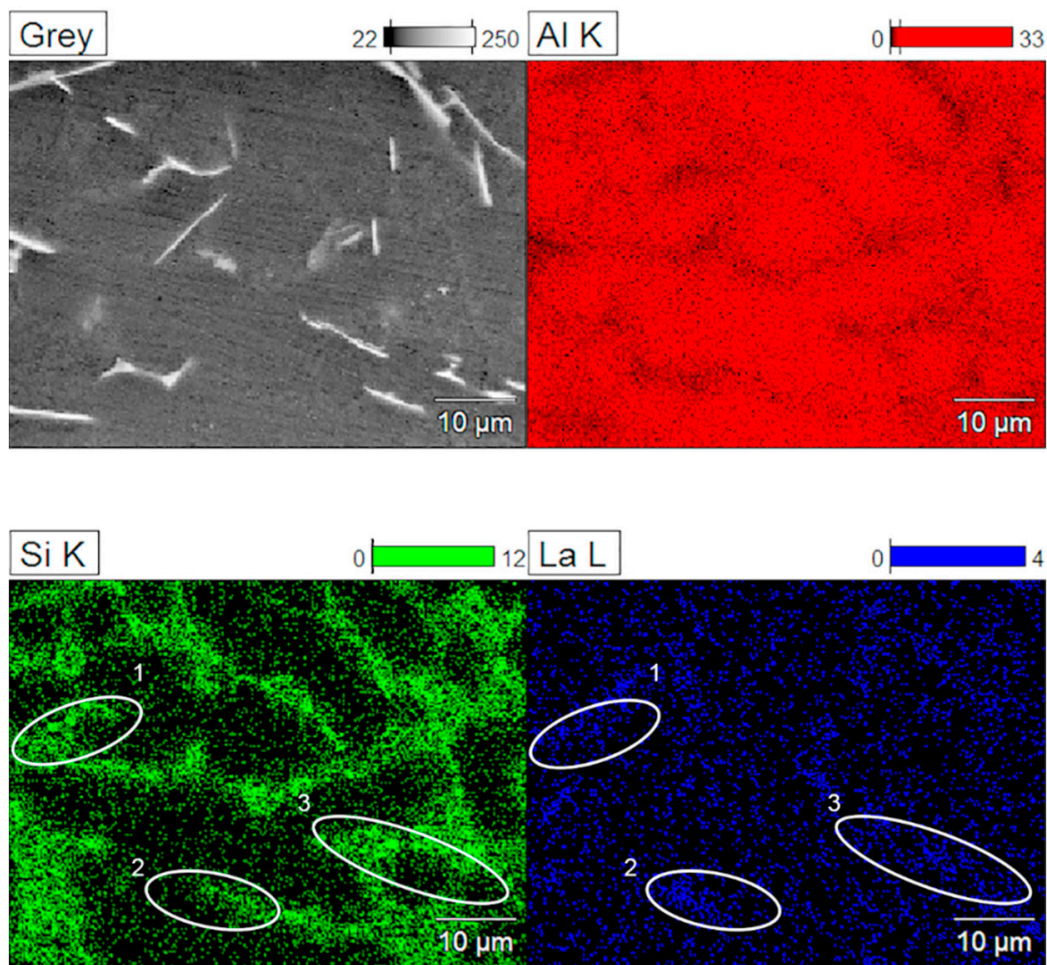


Figure 5. EDS analysis of AlSi5Cu1Mg + 0.9 wt % La alloy.

### 3.2. Wear Rate

The wear rates variation versus the contents of La after a dry sliding distance of 114 m (equivalent to  $600 \text{ s} \times 0.19 \text{ m/s}$ ) is shown in Figure 6. The wear rate was defined as the volume loss of a material by wear per unit sliding distance. Because the wear rate depends just like the friction coefficient on a lot of parameters, this factor is to be found experimentally, and studying the wear mechanism by this quantity is useful in comparing wear rates for different categories of materials. The wear rate of the alloys with La addition were smaller than the matrix alloy, and it could indicate that the alloys with La addition exhibited improved wear resistance compared with the matrix alloy. Then, the AlSi5Cu1Mg + 0.6 wt % La alloys exhibited the least amount of wear rate. In addition, the wear rate of AlSi5Cu1Mg + 0.6 wt % La alloy decreased 48% further than the one of a matrix alloy under the normal load of 1.3 MPa. The effect of the contents of La on wear rate can be explained by using Equation (2) [33] as follows:

$$\text{wear rate} = \frac{kW}{3H}, \quad (2)$$

where  $k$  is the wear coefficient and represents the wear intensity,  $W$  is the normal load, and  $H$  is the average hardness. The addition of rare earth element La made the grain refinement and improved the microhardness of the alloys. Then, the wear rate of the alloys decreased and the wear resistance of the alloys increased.

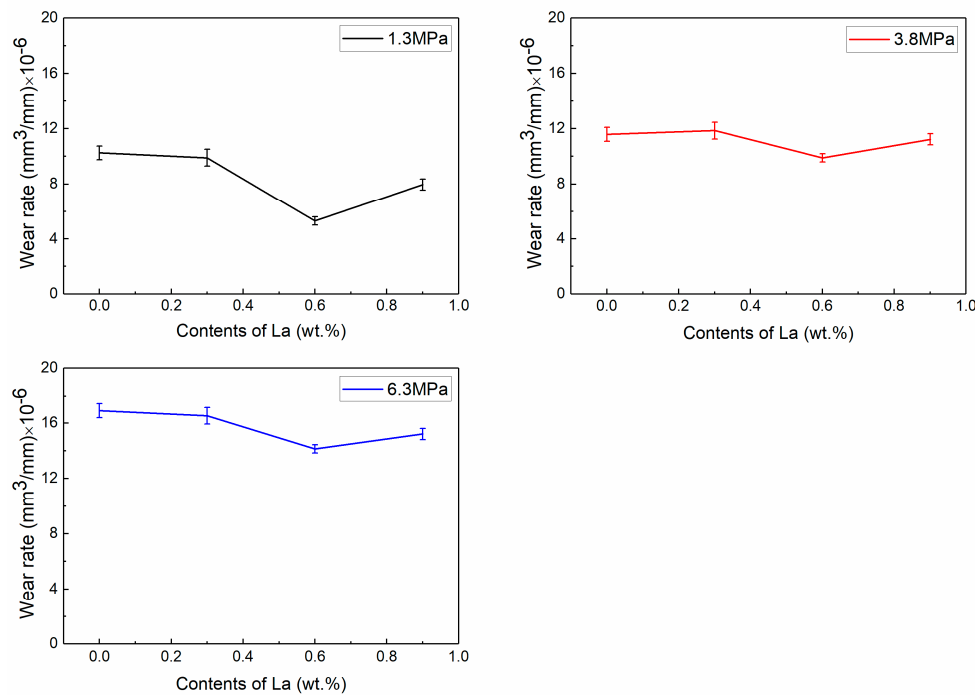


**Figure 6.** Wear rates variation under the normal loads of 1.3, 3.8, 6.3 MPa, and at a sliding velocity of 0.19 m/s versus the contents of La.

The wear rate of the samples under different normal loads at the sliding velocity 0.19 m/s is shown in Figure 7a. As shown, the wear rate was positively correlated with the normal load. It demonstrates that the wear resistance of the alloy deteriorated with increasing normal load. This is consistent with Kaur's experiment [20]. Kaur stated that the change in slope of wear rate vs. normal load curve for as-cast alloy indicates the transition in the mode of wear from mild oxidative regime to severe metallic wear regime. The wear rates of AlSi5Cu1Mg + 0.6 wt % La alloy at different sliding velocity are shown in Figure 7b. With the increase of sliding velocity, the wear rate of alloy increases. It indicates that the wear state of AlSi5Cu1Mg + 0.6 wt % La alloy deteriorates as the increase of friction sliding velocity. This was because the frictional heat generated at a sliding interface. Steady state bulk temperature at the interface is given by Equation (3) [7]:

$$T_b = T_a + \frac{\mu F v \alpha l_b}{A_n k_m}, \quad (3)$$

where  $\mu$  is coefficient of friction;  $F$  is the normal force normal on the pin sample;  $v$  is sliding velocity;  $A_n$  is nominal area of contact;  $\alpha$  is fraction of heat diffusing to pin;  $K_m$  is thermal conductivity;  $T_o$  is sink temperature; and  $l_b$  is mean diffusion distance. When two surfaces slide against each other and work is done against friction, heat is generated at or very close to the sliding interface. This heat energy represents nearly all of the frictional work, since only a small proportion of it is stored in dislocation or other structural defects, or is used in the creation of new surfaces in debris particles or cracks. It is therefore easy to see that there will be a temperature rise near the contact. With the increase of sliding velocity, the temperature of the frictional surface rises. The hardness of metal material usually decreases with the increase of temperature [34].

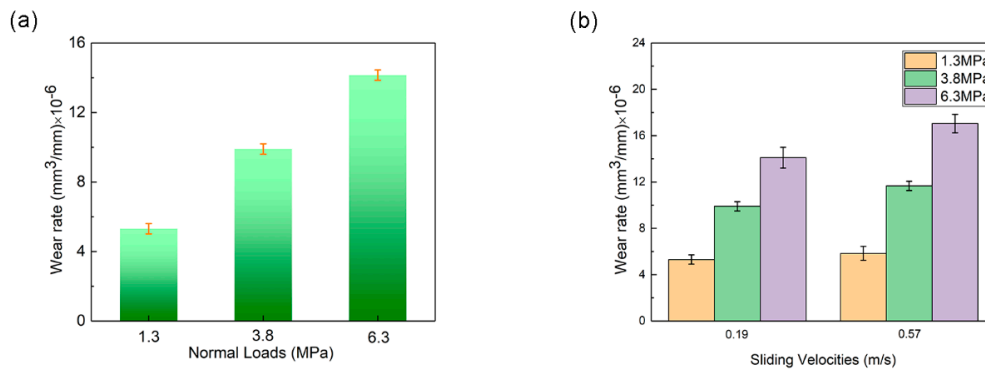


**Figure 7.** Wear rates of AlSi5Cu1Mg + 0.6 wt % La alloy variation (a) at the sliding velocity of 0.19 m/s versus the normal loads; (b) under the normal loads of 1.3, 3.8, 6.3 MPa versus the sliding velocity.

### 3.3. Coefficient of Friction (COF)

The variation of COF as a function of load for AlSi5Cu1Mg + 0 wt %, 0.3 wt %, 0.6 wt %, and 0.9 wt % La at a sliding velocity of 0.19 m/s is depicted in Figure 8; the figure shows that the COF of all alloys increased with the increase of the normal load. For AlSi5Cu1Mg + 0 wt %, 0.3 wt %, 0.6 wt %, 0.9 wt % La alloys, when the normal load increases from 1.3 MPa to 6.3 MPa, the COF increased by 21.4%, 13.5%, 14.7%, 14.3%, respectively. This may be because the real contact area of friction increased as the load increases. When two nominally flat surfaces are placed in contact, surface roughness causes contact to occur at discrete contact asperity. The sum of the areas of all the contact asperity constitutes the real area of contact. When the normal load increases, the height and angle of the asperity flattened because of the plastic deformation. The increase of the actual area leads to an increase in the shear resistance in the rubbing direction.

Then, the COF AlSi5Cu1Mg + 0.6 wt % La alloy vs. sliding velocity test in 1.3, 3.8, 6.3MPa normal load, are shown in Figure 9, respectively. As shown in the figure, when the normal load is consistent, the COF of the alloy decreases as the sliding velocity increases. It can be attributed to the large temperature rise of friction surface because of the raise of the sliding velocity. The high temperature of the friction surface is far more than the recovery and recrystallization temperature of the alloy. Furthermore, it is even possible to bring about dynamic recovery of recrystallization phenomenon [35], due to the fast sliding velocity of friction, then resulting in the grain of friction surface recrystallization and micro-melting. Repeated phase change and deformation, resulting in grain refinement of the top friction surface, so that the COF decreased. Moreover, the decrease in COF with increase in sliding velocity is attributed to two factors [7]: reduced adhesion due to increase oxidation encouraged by high sliding surface temperature caused by localization of the heat and reduced time available for the formation of cold junction at interface, which, in turn, reduces the force required to shear off weld joints at sliding interfaces to maintain the relative motion.

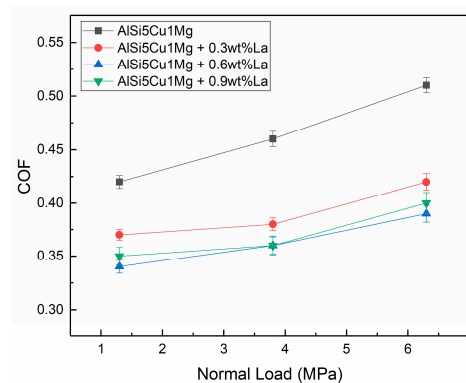


**Figure 8.** The Coefficient of Friction (COF) of alloys at sliding velocity of 0.19 m/s.

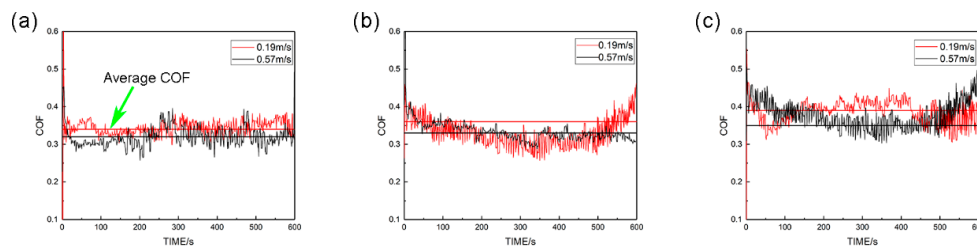


**Figure 9.** Coefficient of friction (COF) of AlSi5Cu1Mg + 0.6 wt % La alloy: (a) 1.3 MPa normal load; (b) 3.8 MPa normal load; (c) 6.3 MPa normal load.

### 3.4. Worn Surfaces

As it can be seen in Figure 10, the scanning electron microscope (SEM) micrographs of worn out surfaces for AlSi5Cu1Mg + 0 wt %, 0.3 wt %, 0.6 wt %, 0.9 wt % La alloys subjected to 0.19 m/s sliding velocity and 3.8 MPa normal load. A lot of valuable information on the mechanism of wear can be provided by studying the worn surfaces [36]. The worn surface of matrix alloy tested at the sliding velocity of 0.19 m/s and the normal load of 3.8 MPa exhibiting parallel grooves and scratches together with rows of furrows and smearing in plastically deformed regions are shown in Figure 10a. These parallel grooves and scratches on the worn surface indicate the occurrence of abrasive wear, which resulted from abrasive contact between the hardened steel disc and aluminium pin. Plastic deformation of surface with rows of furrows is an indicator of adhesive wear. La content increased to 0.3 wt %. As shown in Figure 10b, the shallow craters disappeared, which means that the adhesion wear was reduced. When the content of La increased to 0.6 wt %, the craters on the worn surface almost disappeared, as shown in Figure 10c. It indicates that the wear mechanism of AlSi5Cu1Mg + 0.6 wt % La alloy tested at the sliding velocity of 0.19 m/s and the normal load of 3.8 MPa is mainly abrasive wear because of the maximum hardness, as shown in Figure 4. Nevertheless, by increasing the content of La to 0.9 wt %, as shown in Figure 10d, the adhesive wear appeared again, and the size of the craters is greater. This indicates that the wear mechanism of AlSi5Cu1Mg + 0.9 wt % La alloy tend to be adhesive, due to the deterioration of modification effect. When surfaces come into contact with each other, the films that naturally occur on surfaces often separate the atoms or molecules so there is no tendency for adhesion. However, if the force pushing contacting surfaces becomes sufficient locally at spots in the real area of contact, films can break down and the atoms or molecules of the mating surfaces can make atomic contact and atomic bonding can occur. Then, the surface of the material with less hardness does fall off and stick to the surface of the material with higher hardness. It is called a “metal transfer” [37] phenomenon. Furthermore, the hardness of alloy increases because of the modification by the rare earth element La, the hardness ratio of the steel-disc and the aluminium-pin decreases, so the wear mechanism tends to be abrasive wear, and the adhesive wear tends to be in a secondary position.

The SEM micrographs of worn surfaces for AlSi5Cu1Mg + 0.6 wt % La alloy tested at different conditions are shown in Figure 11. As it can be seen in Figure 11a,b, with the increase of friction load, the characteristics of adhesive wear are more obvious. There is a large proportion of pits in the Figure 11b, and a clear gully is shown in Figure 11a. It was mainly due to rupture of the oxide film (as shown in Figure 11b region A; the EDS analysis of region A is shown in Figure 12) in the friction surface, the new exposed matrix aluminium came into direct contact with the disc under the higher normal load of friction condition. Figure 13 schematically shows the role of normal load for wear. In addition, the hardness of the oxide film was higher than that of the new exposed matrix aluminium. Asperities on the friction plate pierced into the alloys, promoting the formation of pits.

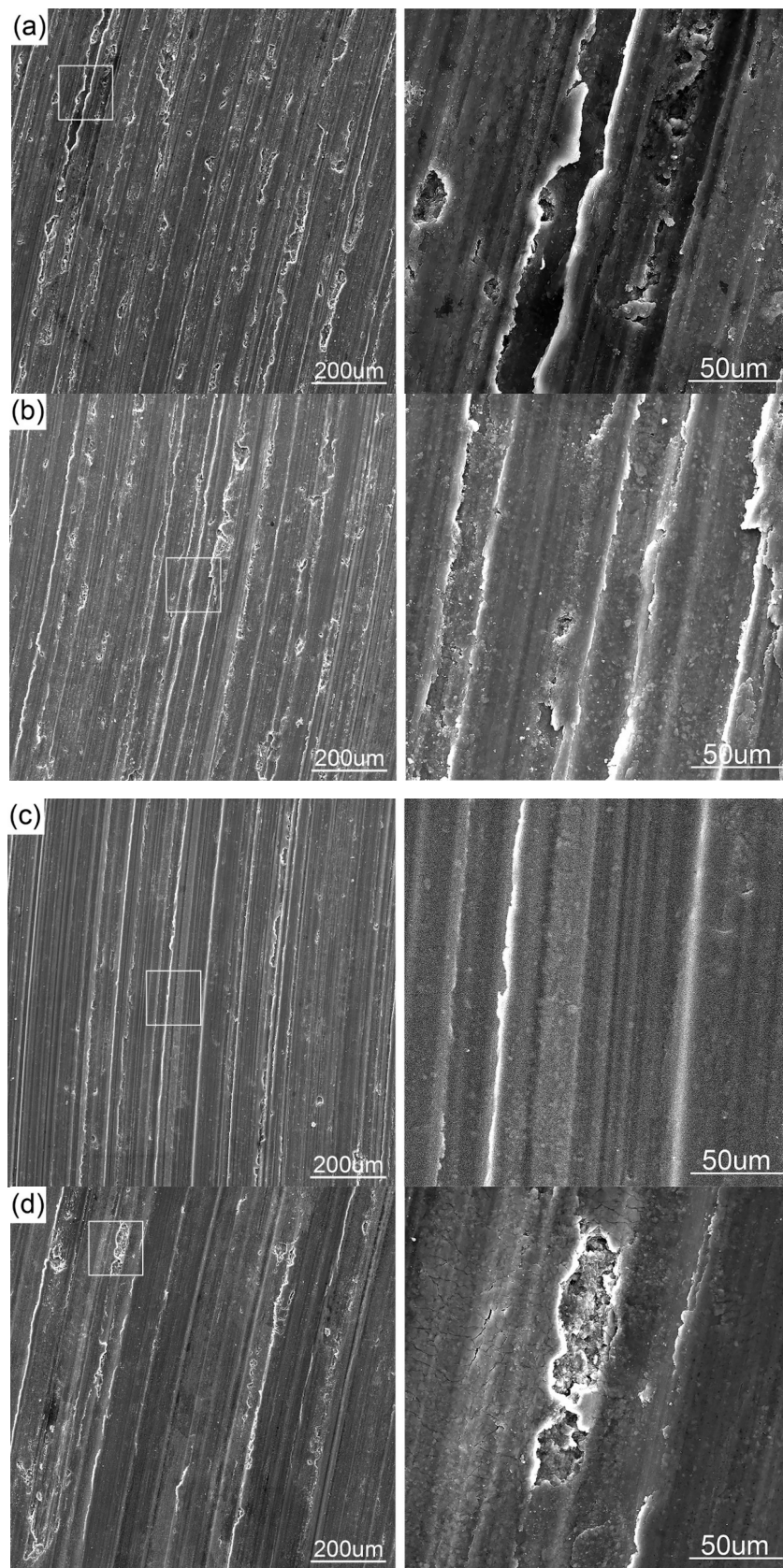


**Figure 10.** SEM micrographs of worn out surfaces for (a) AlSi5Cu1Mg; (b) AlSi5Cu1Mg + 0.3 wt % La; (c) AlSi5Cu1Mg + 0.6 wt % La; (d) AlSi5Cu1Mg + 0.9 wt % La alloys subjected to 0.19m/s sliding velocity and 3.8 MPa normal load, and the high magnification micrographs are on their right side.

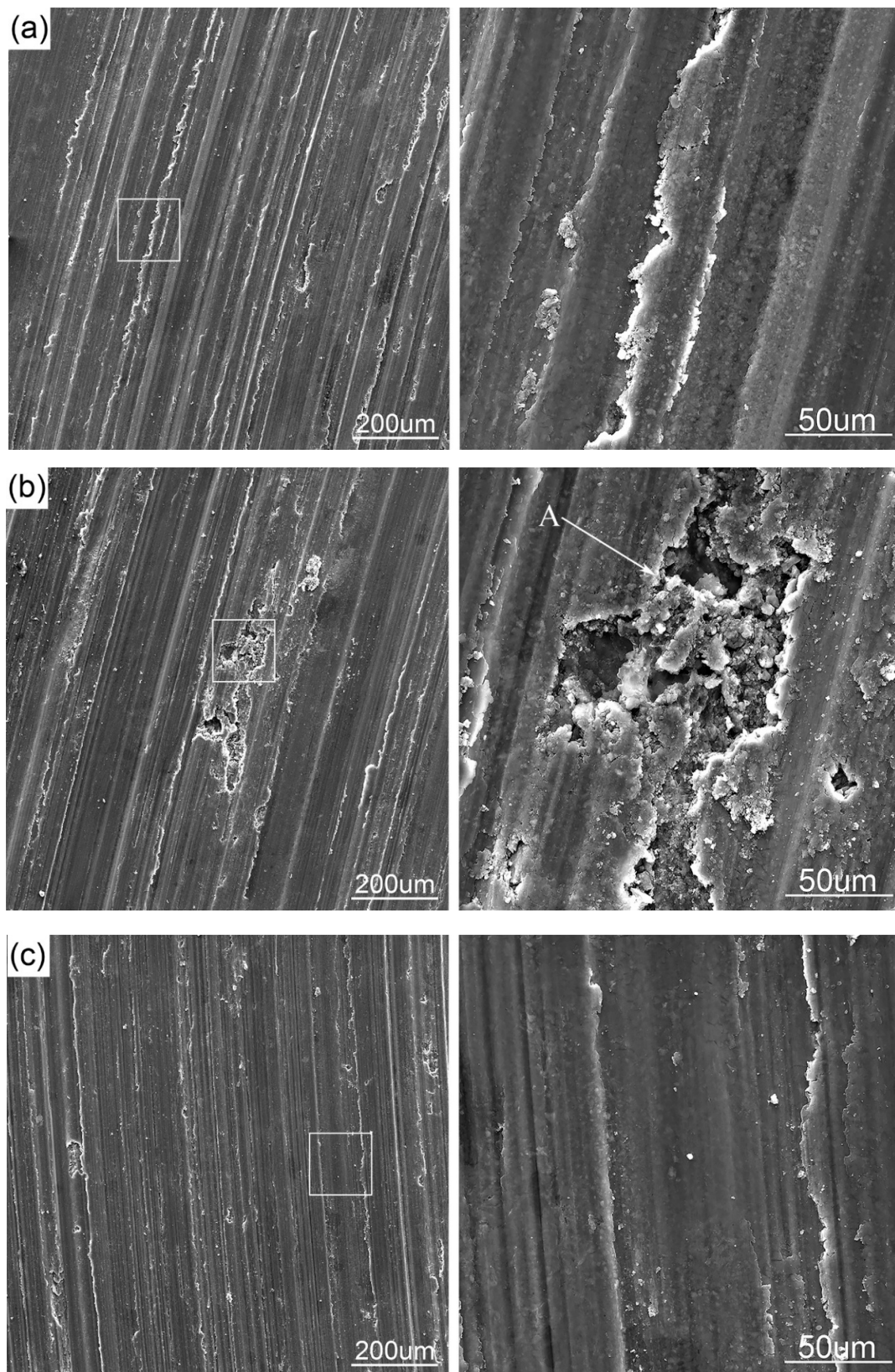


**Figure 11.** SEM micrographs of worn out surfaces for AlSi5Cu1Mg + 0.6 wt % La alloys subjected to: (a) 0.19 m/s sliding velocity and 1.3 MPa normal load; (b) 0.19 m/s sliding velocity and 6.3 MPa normal load; (c) 0.57 m/s sliding velocity and 1.3 MPa normal load, and the high magnification micrographs are on their right side.

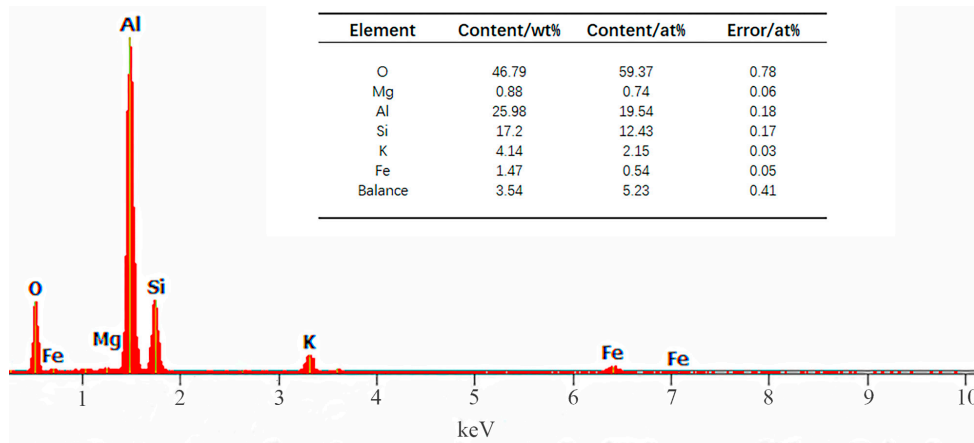


Figure 12. EDS analysis of region A in Figure 11b.

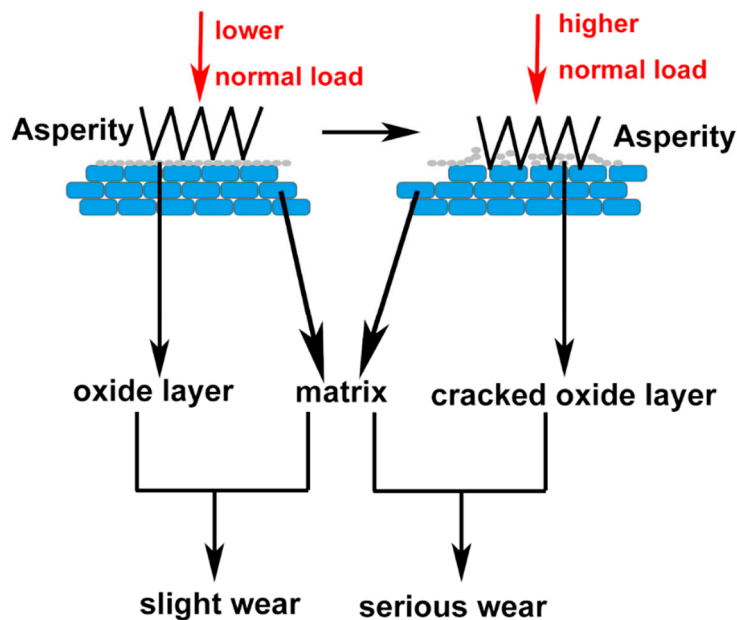


Figure 13. Schematic diagram showing the wear in low normal load and high normal load.

In Figure 11c, there are superficial grooves and scratches together with rows of furrows on the frictional surface. The figure indicates that, with the increase of frictional sliding velocity, the wear mechanism is still abrasive wear; however, the furrows are shallow and the separation distance of the parallel grooves are greater. Because of the high temperature, which is made by the high sliding velocity on the frictional surface, the resulting recrystallization phenomenon happened on the frictional surface, thus refining the grain of the frictional surface and increasing further the hardness of the frictional surface.

#### 4. Conclusions

In summation, we have implemented extensive study on the microstructural, microhardness, wear rate, coefficient of friction and the worn surface of La rare earth element modified AlSi5Cu1Mg alloy. It was notable that adding La rare earth element can improve the microstructure and mechanical properties of the AlSi5Cu1Mg alloy effectively, and the optimum dosage is 0.6 wt %. The AlSi5Cu1Mg + 0.6 wt % La alloy exhibits the most regular grain and smallest grain size and maximum hardness. Therefore, the AlSi5Cu1Mg +0.6 wt % La alloy has the best wear resistance.

Different La rare earth content modification of the AlSi5Cu1Mg alloy shows a different wear mechanism under the same fractional experimental condition (0.19 m/s sliding velocity, 3.8 MPa normal load). The matrix and AlSi5Cu1Mg + 0.9 wt % La alloy manifested severe adhesive wear mechanism; however, the AlSi5Cu1Mg + 0.6 wt % La behaved sharp abrasive wear mechanism and the AlSi5Cu1Mg + 0.3 wt % La alloy is on par with adhesive wear and abrasive wear mechanism. For AlSi5Cu1Mg + 0.6 wt % La alloy, the increase in normal load will promote wear and tear to adhesive wear, and the increase in sliding velocity will weaken the abrasive wear of alloy.

**Acknowledgments:** This research is supported by the National Natural Science Foundation of China (51364035) and the Natural Science Foundation of Jiangxi Province (20171BAB206034).

**Author Contributions:** Wei Liu and Hong Yan conceived and designed the experiments; Wei Liu and Hong Yan performed the experiments; Wei Liu, Hong Yan and Jian-Bin Zhu analyzed the data; Wei Liu, Hong Yan and Jian-Bin Zhu contributed reagents/materials/analysis tools; Wei Liu, Hong Yan and Jian-Bin Zhu wrote the paper.

**Conflicts of Interest:** The author declares no conflict of interest.

## References

- Costa, S.; Moura, A.D.; Esteves, A.; Barbosa, J.; Pinto, A.M.P.; Braga, M.H. Simulation of the nucleation of the precipitate Al<sub>3</sub>Sc in an aluminum scandium alloy using molecular dynamics and kinetic Monte Carlo method. *J. Am. Chem. Soc.* **2013**, *129*, 4670–14683.
- Baradeswaran, A.; Perumal, A.E. Wear and mechanical characteristics of Al 7075/graphite composites. *Compos. Part B Eng.* **2014**, *56*, 472–476. [[CrossRef](#)]
- Rodríguez, J.; Poza, P.; Garrido, M.A.; Rico, A. Dry sliding wear behaviour of aluminium–lithium alloys reinforced with SiC particles. *Wear* **2007**, *262*, 292–300. [[CrossRef](#)]
- Senthilkumar, M.; Saravanan, S.D.; Shankar, S. Dry sliding wear and friction behavior of aluminum-rice husk ash composite using Taguchi's technique. *J. Compos. Mater.* **2015**, *49*, 2241–2250. [[CrossRef](#)]
- Dinakaran, I.; Nelson, R.; Vijay, S.J.; Akinlabi, E.T. Microstructure and wear characterization of aluminum matrix composites reinforced with industrial waste fly ash particulates synthesized by friction stir processing. *Mater. Charact.* **2016**, *118*, 149–158. [[CrossRef](#)]
- Sannino, A.P.; Rack, H.J. Dry sliding wear of discontinuously reinforced aluminum composites: Review and discussion. *Wear* **1995**, *189*, 1–19. [[CrossRef](#)]
- Dwivedi, D.K. Adhesive wear behaviour of cast aluminium–silicon alloys: Overview. *Mater. Des.* **2010**, *31*, 2517–2531. [[CrossRef](#)]
- Shipway, P.H.; Kennedy, A.R.; Wilkes, A.J. Sliding wear behaviour of aluminium-based metal matrix composites produced by a novel liquid route. *Wear* **1998**, *216*, 160–171. [[CrossRef](#)]
- Miyajima, T.; Iwai, Y. Effects of reinforcements on sliding wear behavior of aluminum matrix composites. *Wear* **2003**, *255*, 606–616. [[CrossRef](#)]
- Soy, U.; Ficici, F.; Demir, A. Evaluation of the Taguchi method for wear behavior of Al/SiC/B<sub>4</sub>C composites. *J. Compos. Mater.* **2012**, *46*, 851–859. [[CrossRef](#)]
- Maleque, A.; Karim, R. Wear behavior of as-cast and heat treated triple particle size SiC reinforced aluminum metal matrix composites. *Ind. Lubr. Tribol.* **2009**, *61*, 78–83. [[CrossRef](#)]
- Altınkök, N. Investigation of mechanical and machinability properties of Al<sub>2</sub>O<sub>3</sub>/SiCp reinforced Al-based composite fabricated by stir cast technique. *J. Porous Mater.* **2015**, *22*, 1643–1654. [[CrossRef](#)]
- Selvi, S.; Rajasekar, E. Theoretical and experimental investigation of wear characteristics of aluminum based metal matrix composites using RSM. *J. Mech. Sci. Technol.* **2015**, *29*, 785–792. [[CrossRef](#)]
- Ficici, F.; Koksal, S. Microstructural characterization and wear properties of in situ AlB<sub>2</sub>-reinforced Al-4Cu metal matrix composite. *J. Compos. Mater.* **2016**, *50*, 1685–1696. [[CrossRef](#)]
- Mishra, R.S.; Valiev, R.Z.; Mcfadden, S.X.; Islamgaliev, R.K.; Mukherjee, A.K. Severe plastic deformation processing and high strain rate superplasticity in an aluminum matrix composite. *Scr. Mater.* **1999**, *40*, 1151–1155. [[CrossRef](#)]
- Jun, J.; Kim, J.; Park, B.K.; Kim, K.; Jung, W. Effects of rare earth elements on microstructure and high temperature mechanical properties of ZC63 alloy. *J. Mater. Sci.* **2005**, *40*, 2659–2661. [[CrossRef](#)]

17. Liu, Y.L.; Luo, L.; Shun, M.Z.; Zhang, L.; Zhao, Y.H.; Wu, B.L. Microstructure and mechanical properties of Al–5.5Fe–1.1V–0.6Si alloy solidified under near-rapid cooling and with Ce addition. *Rare Met.* **2016**, *1–6*. [[CrossRef](#)]
18. Chang, J.; Moon, I.; Choi, C. Refinement of Cast Microstructure of Hypereutectic Al–Si Alloys through the Addition of Rare Earth Metals. *J. Mater. Sci.* **1998**, *33*, 5015–5023. [[CrossRef](#)]
19. Qiu, H.; Yan, H.; Hu, Z. Effect of samarium (Sm) addition on the microstructures and mechanical properties of Al–7Si–0.7Mg alloys. *J. Alloys Compd.* **2013**, *567*, 77–81. [[CrossRef](#)]
20. Kaur, P.; Dwivedi, D.K.; Pathak, P.M.; Rodriguez, S.H. The effect of electromagnetic stirring and cerium addition on dry sliding reciprocating wear of hypereutectic aluminium–silicon alloy. *Proc. Inst. Mech. Eng. Part J J. Eng. Tribol.* **2011**, *226*, 251–258. [[CrossRef](#)]
21. Farias, M.C.M.; Souza, R.M.; Sinatora, A.; Tanaka, D.K. The influence of normal load, sliding velocity and martensitic transformation on the unlubricated sliding wear of austenitic stainless steels. *Wear* **2007**, *263*, 773–781. [[CrossRef](#)]
22. Kim, H.J.; Emge, A.; Karthikeyan, S.; Rigney, D.A. Effects of tribooxidation on sliding behavior of aluminum. *Wear* **2005**, *259*, 501–505. [[CrossRef](#)]
23. Yan, H.; Ye, H.Y.; Chen, W. Dry friction and wear performance of co-continuous Al–23Si/SiC composites. *Mater. Res. Innov.* **2015**, *19*, 131–135. [[CrossRef](#)]
24. Uyyuru, R.K.; Surappa, M.; Brusethaug, S. Tribological behavior of Al–Si–SiC composites/automobile brake pad system under dry sliding conditions. *Tribol. Int.* **2007**, *40*, 365–373. [[CrossRef](#)]
25. Mrowkanowotnik, G.; Sieniawski, J.; Nowotnik, A. The chemical phenol extraction of intermetallic particles from casting AlSi5Cu1Mg alloy. *J. Microsc.-Oxf.* **2010**, *237*, 407–410. [[CrossRef](#)] [[PubMed](#)]
26. Yi, Y.; Fan, Y.G.; Tang, Y.J. Effect of lanthanum-praseodymium-cerium mischmetal on mechanical properties and microstructure of Mg–Al alloys. *J. Wuhan Univ. Technol.* **2011**, *26*, 102–104. [[CrossRef](#)]
27. Zhang, J.H.; Liu, K.; Fang, D.; Qiu, X.; Tang, D.X.; Meng, J. Microstructure, tensile properties, and creep behavior of high-pressure die-cast Mg–4Al–4RE–0.4Mn (RE = La, Ce) alloys. *J. Mater. Sci.* **2009**, *44*, 2046–2054. [[CrossRef](#)]
28. Asl, K.M.; Masoudi, A.; Khomamizadeh, F. The effect of different rare earth elements content on microstructure, mechanical and wear behavior of Mg–Al–Zn alloy. *Mater. Sci. Eng. A Struct.* **2010**, *527*, 2027–2035.
29. Hall, E.O. The Deformation and Ageing of Mild Steel: II Characteristics of the Lüders Deformation. *Proc. Phys. Soc.* **1951**, *64*, 742. [[CrossRef](#)]
30. Petch, N.J. The Cleavage Strength of Polycrystals. *J. Iron Steel Inst.* **1953**, *174*, 25–28.
31. Tiryakioğlu, M. On the relationship between Vickers hardness and yield load in Al–Zn–Mg–Cu Alloys. *Mater. Sci. Eng. A Struct.* **2015**, *633*, 17–19. [[CrossRef](#)]
32. Pournabari, B.; Emamy, M. Effects of La intermetallics on the structure and tensile properties of thin section gravity die-cast A357 Al alloy. *Mater. Des.* **2016**, *94*, 111–120. [[CrossRef](#)]
33. Yang, L.J. Wear coefficient equation for aluminium-based matrix composites against steel disc. *Wear* **2003**, *255*, 579–592. [[CrossRef](#)]
34. Elsalam, F.A.; Wahab, L.A.; Nada, R.H.; Zahran, H.Y. Temperature and dwell time effect on hardness of Al-base alloys. *J. Mater. Sci.* **2007**, *42*, 3661–3669.
35. Tahamtan, S.; Halvaeae, A.; Emamy, M. The influences of interfacial characteristics and subsurface microstructural evolution on wear behavior of Al/A206-5 Pct alumina micro/nano-composites. *Metall. Mater. Trans. B* **2015**, *46*, 1115–1124. [[CrossRef](#)]
36. Bhushan, B.; Ko, P.L. *Introduction to Tribology*, 2nd ed.; John Wiley & Sons Inc.: New York, NY, USA, 2002.
37. Fishkis, M. Metal transfer in the sliding process. *Wear* **1988**, *127*, 101–110. [[CrossRef](#)]

